CENTRAL RESEARCH LIBRARY
DOCUMENT COLLECTION

1

OAK RIDGE NATIONAL LABORATORY
operated by
UNION CARBIDE CORPORATION
NUCLEAR DIVISION
for the
U.S. ATOMIC ENERGY COMMISSION

OAK RIDGE NATIONAL LABORATORY LIBRARIES
3 4456 0549822 6

ORNL-TM-2074

PRELIMINARY STUDY OF PYROLYTIC TUNGSTEN DEPOSITION

D. O. Hobson

OAK RIDGE NATIONAL LABORATORY
CENTRAL RESEARCH LIBRARY
DOCUMENT COLLECTION
LIBRARY LOAN COPY
DO NOT TRANSFER TO ANOTHER PERSON
If you wish someone else to see this document, send in name with document and the library will arrange a loan.
UCN-7969
(3 3-67)

NOTICE This document contains information of a preliminary nature and was prepared primarily for internal use at the Oak Ridge National Laboratory. It is subject to revision or correction and therefore does not represent a final report.

LEGAL NOTICE

This report was prepared as an account of Government sponsored work. Neither the United States, nor the Commission, nor any person acting on behalf of the Commission:

A. Makes any warranty or representation, expressed or implied, with respect to the accuracy, completeness, or usefulness of the information contained in this report, or that the use of any information, apparatus, method, or process disclosed in this report may not infringe privately owned rights; or

B. Assumes any liabilities with respect to the use of, or for damages resulting from the use of any information, apparatus, method, or process disclosed in this report.

As used in the above, "person acting on behalf of the Commission" includes any employee or contractor of the Commission, or employee of such contractor, to the extent that such employee or contractor of the Commission, or employee of such contractor prepares, disseminates, or provides access to, any information pursuant to his employment or contract with the Commission, or his employment with such contractor.

ORNL-TM-2074

Contract No. W-7405-eng-26

METALS AND CERAMICS DIVISION

PRELIMINARY STUDY OF PYROLYTIC TUNGSTEN DEPOSITION

D. O. Hobson

JANUARY 1968

OAK RIDGE NATIONAL LABORATORY
Oak Ridge, Tennessee
operated by
UNION CARBIDE CORPORATION
for the
U.S. ATOMIC ENERGY COMMISSION

OAK RIDGE NATIONAL LABORATORY LIBRARIES
3 4456 0549822 6

FOREWORD

This work constitutes research and development accomplished by the author over the period of November 1964 to June 1965 and reflects the many unknowns present in the initial studies of chemical vapor deposition.

CONTENTS

	Page
Abstract	1
Introduction	1
General Comments	2
Equipment and Experimental Procedures	5
Results	10
Pressure Effects	10
Ratio Effects	12
Composition Effects on Nodule Formation	16
Extrapolation and Theory	24
Pressure and Envelope Curves	26
Effects of Type of Gas Flow Pattern	32
Conclusions	35
Acknowledgments	36

PRELIMINARY STUDY OF PYROLYTIC TUNGSTEN DEPOSITION

D. O. Hobson

ABSTRACT

The objective of this work was the development of a better understanding of the process of pyrolytic tungsten deposition. We were able to optimize deposition pressures, flow rates, and H_2/WF_6 ratios for specific mandrel sizes and a specific mandrel temperature. Deposition efficiency varied with both pressure and gas ratio. Total flow rates, WF_6 flow rates, amount deposited, and efficiency were correlated, and the correlations are presented graphically.

X-ray diffraction showed the deposits to be preferentially oriented in the growth direction. Analysis of the data indicated that the tendency for nodular growth was a direct function of gas composition.

The results of the experimental part of this work were extrapolated to produce working hypotheses for predicting the behavior of tungsten deposition under a variety of conditions.

INTRODUCTION

The purpose of this work was to begin to rationalize and reconcile the interactions among the various conditions for tungsten deposition and to make the process more amenable to prediction and theory. Like any new technology, vapor deposition of tungsten is not well understood. Certain deposition parameters have often been chosen for various reasons, then studied over a limited range to obtain the most satisfactory deposit. However, a comprehensive study involving a wide range of variables had not been made.

Basic interrelationships among the deposition parameters are lacking in the overall picture. For example, deposition parameters determined to give a "good" deposit in a small tube furnace with a 20-in.^{2} mandrel surface probably would not produce a similar deposit on a 300-in.^{2} surface,

even though scaled to the larger system. A knowledge of the interactions among variables, therefore, might allow extrapolation to the larger system without the necessity for repetitive parameter redetermination.

This report is labeled "preliminary" because time did not permit us to cover the ranges of parameters we had hoped to study. Chiefly lacking are data for larger mandrels and for greater reactant gas flow rates. However, on the basis of the results obtained a deposition model is presented that will allow extrapolation to larger systems. This report is also "preliminary" to the extent that no attempt was made to determine the mechanism of deposition. Several possible mechanisms are proposed. Previous demonstration of deposition feasibility has been reported,[1] and subsequent studies are summarized.[2,3]

This report consists of two main sections: One deals with the experimental procedures and results, and the other with inferences drawn from the data and theories postulated through extrapolation of the available data.

GENERAL COMMENTS

Chemical vapor deposition of tungsten involves the reduction of WF_6 gas by hydrogen on a heated substrate usually at or below atomspheric pressure. The overall reaction is $WF_6 + 3H_2 \rightarrow W + 6HF$. Such factors as diffusion of reacting components, composition changes in the reacting gases during deposition, and temperature effects on deposition rate are related to the deposition parameters.

---

[1]R. L. Heestand, J. I. Federer, and C. F. Leitten, Jr., Preparation and Evaluation of Vapor-Deposited Tungsten, ORNL-3662 (August 1964).

[2]C. F. Leitten, Jr., F. H. Patterson, W. C. Robinson, Jr., J. E. Spruiell, and B. F. Shuler, Metals and Ceramics Div. Ann. Progr. Rept. June 30, 1966, ORNL-3970, pp. 85–89.

[3]W. R. Martin, R. L. Heestand, and W. C. Robinson, Jr., Metals and Ceramics Div. Ann. Progr. Rept. June 30, 1967, ORNL-4170, pp. 81–84.

Temperature strongly affects deposition rate as a function of mandrel length in a tubular mandrel.[1] The higher the temperature, the faster the deposit is formed. Increasing the deposition temperature from 500 to 1000°C increased the rate by a factor of 7 and shifted the location of the maximum deposit thickness from the midpoint of the mandrel to a point closer to the gas inlet. Possible reasons for these effects are an increase in the reaction rate, an increase in the diffusion rate of the reacting components, and changes in surface chemisorption. Realizing that temperature plays an important part in controlling thickness distribution, and knowing that Heestand and co-workers[1] had investigated gross temperature effects, we held temperature nominally constant in this study and concentrated on the other variables. Changes in mass flow rate, reacting gas ratios, and pressure affect the temperature profile along the mandrel. These effects are probably small and were ignored in the present work.

Nodular growths resembling cones have been observed in tungsten deposits. These cones appear to be nucleated at or near the substrate and may be related to changes in the composition of the reacting gases at the gas-metal interface. Such a dependence on deposit morphology was found by Campbell[4] in a study of the formation of Al_2O_3 fibers by a halide pyrohydrolysis process. Quoting Campbell, "The relative degrees of supersaturation associated with the three principle growth forms (whiskers, single crystals, and powders) have been described as follows: A very low degree of supersaturation is required for whisker growth, whereas a medium degree of supersaturation supports single-crystal growth. Powders form at high supersaturation by spontaneous precipitation in the gas phase."

Campbell does not define supersaturation, but the term probably refers to the concentration of halide in the gas stream. Thus, a change in the gas composition could cause a change in the structure of the deposit.

---

[4]W. B. Campbell, Feasibility of Forming Refractory Fibers by a Continuous Process, 3rd Quart. Progr. Rept. Aug. 25 to Nov. 25, 1963, AMRA-CR-63-03/3.

J. D. Fleming,[5] asked to comment on Campbell's supersaturation concept, did so with the understanding that much of what he said was highly speculative and based on no experimental data whatsoever. "Definition of the supersaturation based on the degree of departure from equilibrium does not seem illogical, since a measure of this type should relate directly to the process of nucleation. If the reacting mixture is far displaced from equilibrium, the survival rates of the nuclei would be high, and stable nucleation would occur even at unfavorable nucleation sites, leading in extreme circumstances to the formation of powder in the vapor space. A lower degree of displacement would decrease the rate of nucleus survival and stable nucleation would not occur at unfavorable sites. Any favorable site would still show a tendency toward nucleation, but the rate would be dependent on the energy of the growth plane. At still lower displacement from equilibrium, stable nucleation and growth would occur only on the most favorable sites. Under these conditions, low-energy planes would tend to grow at the expense of loss of deposit from any preexisting, higher energy planes through the mechnnism of the reversible vapor-phase reaction. This would lead to highly oriented, probably coarsely crystalline deposits or even to whiskers."

The above discussion is thermodynamically sound and may be applicable to Campbell's findings but can only be conjecturally applied to the present study. In fact, the above comments apply only if there is a change in growth plane in going from one type of deposit to another. The growth planes will be examined later in this report. Intuitively, pressure might have at least three major effects on the deposition process. The reaction, $WF_6 + 3H_2 \rightarrow W + 6HF$, proceeds to the right with an increase in the number of gas molecules. A decrease in the system pressure should favor completion of the reaction. A decrease in the pressure should also increase the mean free path of the molecules and thus favor increased diffusion rates. On the other hand, decreasing the pressure in a small mandrel would cause a large increase in the velocity of the gases in the tube, decrease the time available for reaction, and possibly decrease efficiency.

---

[5]J. D. Fleming, Consultant from Georgia Institute of Technology, Letter to R. L. Heestand, Aug. 15, 1964.

Variations in the ratio of hydrogen to WF_6 can also affect the deposition of tungsten. Too low a ratio can decrease the deposition rate due both to the lack of sufficient hydrogen to consume the WF_6 and to the inability of the hydrogen to diffuse rapidly enough to reach the reaction surface. Too high a ratio at a particular pressure could raise the velocity of the gases relative to the substrate and not allow time for the components to react. Although stoichiometric considerations call for three moles of hydrogen per mole of WF_6, factors such as geometry, diffusion rate, and kinetics have important effects, which override stoichiometric considerations and require an excess of hydrogen in the system for optimum deposition.

EQUIPMENT AND EXPERIMENTAL PROCEDURES

The deposition apparatus is illustrated in Fig. 1 and schematically in Fig. 2. Clamshell resistance furnaces were controlled by Wheelco proportional controllers calibrated for Chromel versus Alumel thermocouples. The substrate material was copper tubing joined at each end of the furnace to thin-walled stainless steel tubing to minimize heat losses. A Hastings mass flowmeter measured the WF_6 flow rate, and a conventional glass floating-ball Brooks flowmeter measured the hydrogen flow rate. The hydrogen flowmeter was calibrated with air against a Precision wet test meter and then converted by an appropriate factor to indicate hydrogen flow rates. The Hastings meter was calibrated by comparing the weight change of the WF_6 supply cylinder with the indicated amount of WF_6 transferred.

Since the deposition process was not 100% efficient, WF_6 that passed the primary deposition section was reduced to tungsten in an 800°C scavenger furnace to minimized WF_6 contamination of the vacuum pump. A gas ballast mechanical pump was used for the initial system evacuation and for removal of the reaction products, including excess hydrogen, hydrogen fluoride, and small amounts of unreacted WF_6. Other equipment items included a mercury manometer to measure the system pressure, a cold trap to prevent backstreaming of vacuum pump oil vapor, and a countercurrent water scrubber to remove hydrogen fluoride from the effluent gas stream.

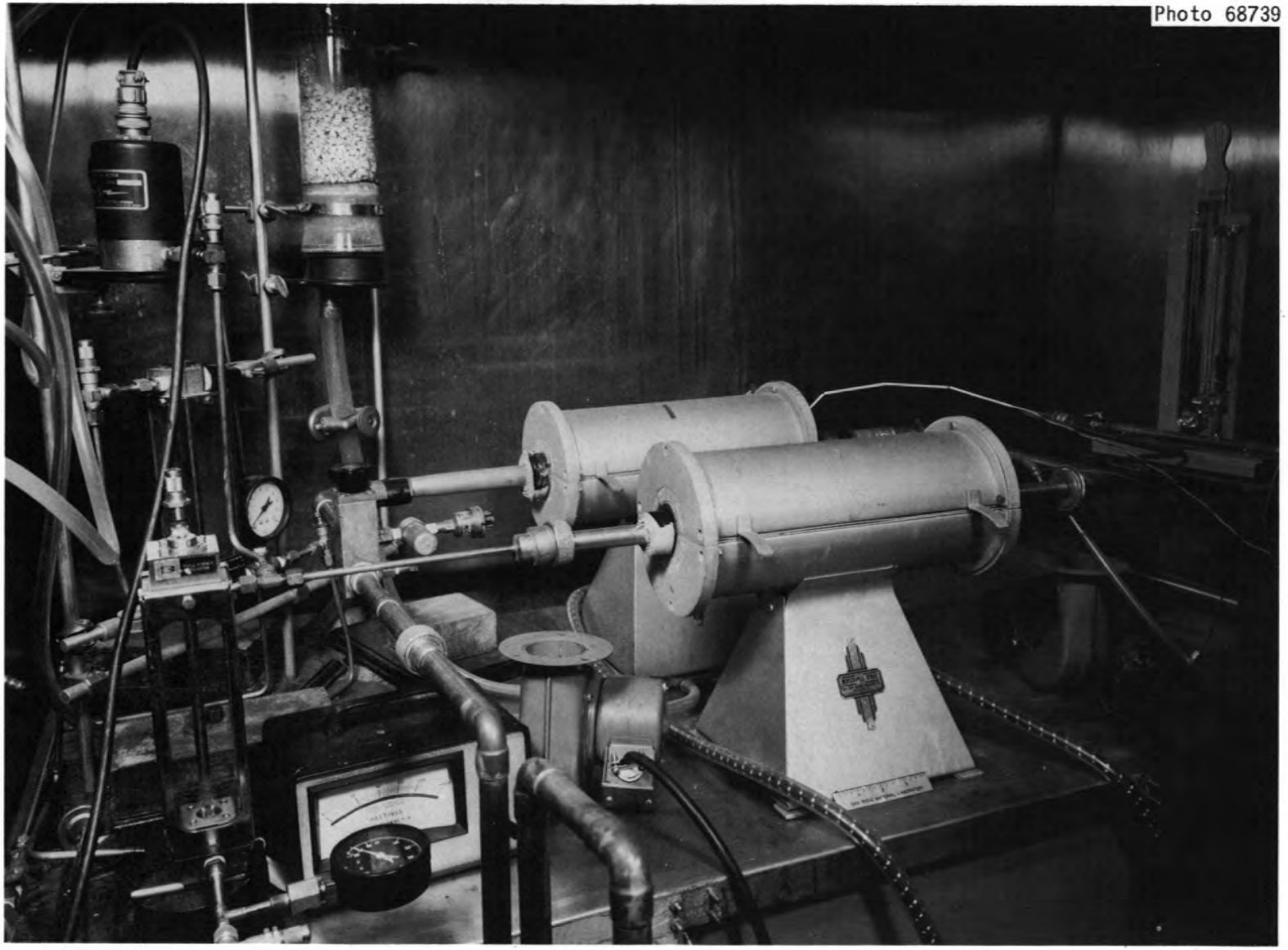

Fig. 1. Experimental Setup for Pyrolytic Tungsten Deposition.

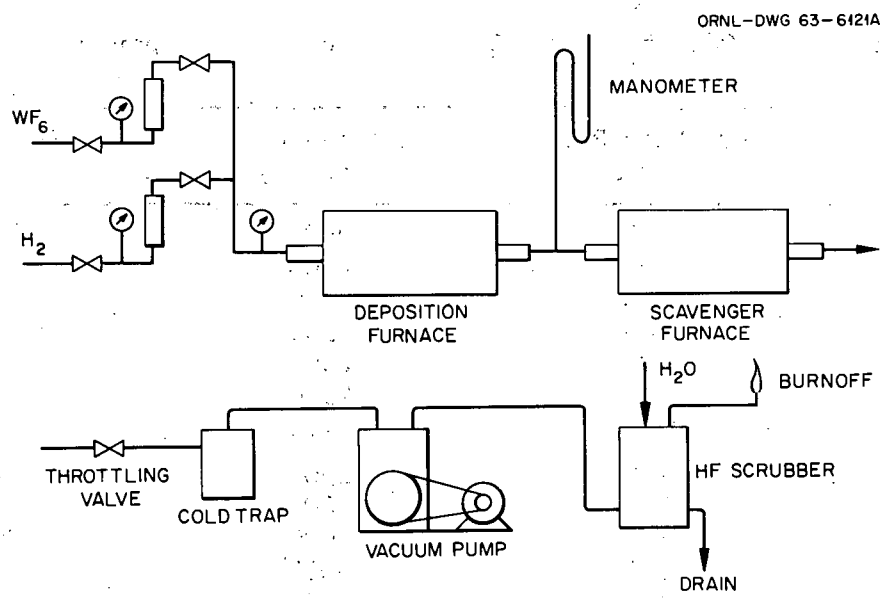

Fig. 2. Tungsten Deposition Apparatus.

In a typical experiment, the deposition furnace and the scavenger furnace were raised to temperature with the cold trap filled and hydrogen flowing to ensure a clean surface on the copper mandrel. The system pressure was adjusted by a throttling valve ahead of the vacuum pump. Then WF_6 was admitted, the pressure was readjusted if necessary, and the deposition was carried out under constant temperature, pressure, and inlet composition of the reacting gases. At the completion of deposition, the flow of WF_6 was stopped and the system was cooled to room temperature under hydrogen. As shown in Table 1, 28 deposition experiments were conducted under different conditions of pressure, WF_6 flow rate, H_2/WF_6 ratio, and mandrel size. The H_2/WF_6 ratio ranged from 6 to 62 and the mandrel size from 5/8 to 1 in. ID.

The amount of tungsten deposited was calculated from thickness measurements. The copper mandrel was dissolved in a hot nitric acid solution, and the resulting tungsten tube was sectioned into 2-in.-long pieces with a water-cooled abrasive cutoff wheel. Thicknesses were then measured to the nearest 0.0005 in. with a micrometer. The thicknesses were plotted as a function of position along the tube, and the area under the curve was graphically integrated. This is the area of a longitudinal cross section of the deposit and is a useful measure of the amount of

Table 1. Conditions of Tungsten Deposition Experiments[a]

Run	WF_6 Flow Rate (cc/min)	H_2 Flow Rate (cc/min)	Pressure (torr)
9	100	2500	10
4	100	2500	20
5	100	2500	30
6	100	2500	40
10	100	2500	50
11	100	2500	60
16	100	700	10
17	100	1500	10
13	100	1000	20
12	100	3000	20
27	100	3000[b]	20
14	100	3500	20
2	40	2500	20
30	80	2020	20
31	100	2000	20
29	200	1900	20
32	200	1900	20
33	200	1900	20
34	200	3000	20
28	300	1800	20
18	100	1500	30
22	100	1500	30
19	100	2000	30
20	100	3000	30
21	100	3500	30
24	100	2000	40
26	100	2250	40
15	100	3100	40

[a]Temperature 600°C measured at the mandrel midpoint. Time: 5 hr. Nominal 12-in. mandrel length.

[b]Plus 500 cc/min argon.

tungsten deposited. The volumes of the deposits were calculated by standard methods of calculus and converted to weight of tungsten with the density taken as 19.3 g/cc. The results of these calculations are shown in Table 2. The 2-in.-long sections allowed examination of the inside surface of the tubes for nodulation.

Table 2. Results of Weight Calculations

Run	Longitudinal Area (in.^{2})	Volume (in.^{3})	Volume (cm^3)	Tungsten (g)	Mole Ratio H_2/WF_6	Pressure (torr)
2	0.126	0.309	5.064	97.7	62.5	20
4	0.298	0.741	12.14	234.3	25	20
5	0.324	0.799	13.09	252.6	25	30
6	0.318	0.773	12.67	244.5	25	40
7	0.298	0.727	11.91	229.9	20	20
8	0.201	0.501	8.21	158.4	15	20
9	0.146	0.360	5.90	113.9	25	10
10	0.288	0.723	11.85	228.7	25	50
11	0.302	0.744	12.19	235.3	25	60
12	0.192	0.481	7.88	152.1	30	20
13	0.132	0.332	5.44	105.0	10	20
14	0.217	0.540	8.85	170.8	35	20
15	0.185	0.461	7.56	145.9	31	40
16	0.122	0.307	5.03	97.1	7	10
17	0.123	0.310	5.08	98.0	15	10
18	0.230	0.572	9.37	180.8	15	30
19	0.184	0.461	7.56	145.9	20	30
20	0.233	0.578	9.47	182.8	30	30
21	0.234	0.581	9.52	183.7	35	30
22	0.195	0.487	7.98	154.0	15	30
24	0.281	0.695	11.39	219.8	20	40
26	0.302	0.738	12.10	233.5	22.5	40
27	0.268	0.664	10.88	210.0	30	20
28	0.266	0.658	10.78	208.0	6	20
29	0.283	0.699	11.46	221.2	9.5	20
30	0.257	0.635	10.41	200.9	25.2	20
31	0.256	0.715	11.72	226.2	9.5	20
32	0.291	0.810	13.26	255.9	9.5	20
33	0.263	0.831	13.62	262.9	9.5	20
34	0.204	0.648	10.62	204.9	15	20

RESULTS

Pressure Effects

Six runs were made at 100 cc/min WF_6, 2500 cc/min H_2, 600°C, and 5-hr duration. The pressure was varied from 10 to 60 torr. The results of these runs are plotted in Fig. 3 as deposit wall thickness versus position along the tube. There are large differences with deposition pressure in the amount of tungsten deposited and in the distribution of the deposited tungsten. The 10-torr run gave a relatively thin deposit with a maximum thickness of approximately 18 mils and a longitudinal area of 0.146 in.^{2}. The 20-torr run showed twice as much deposit as the 10-torr run. The thickness increased to a maximum of 37 mils and the area to 0.298 in.^{2}. The 30-torr run resulted in a further increase in deposited

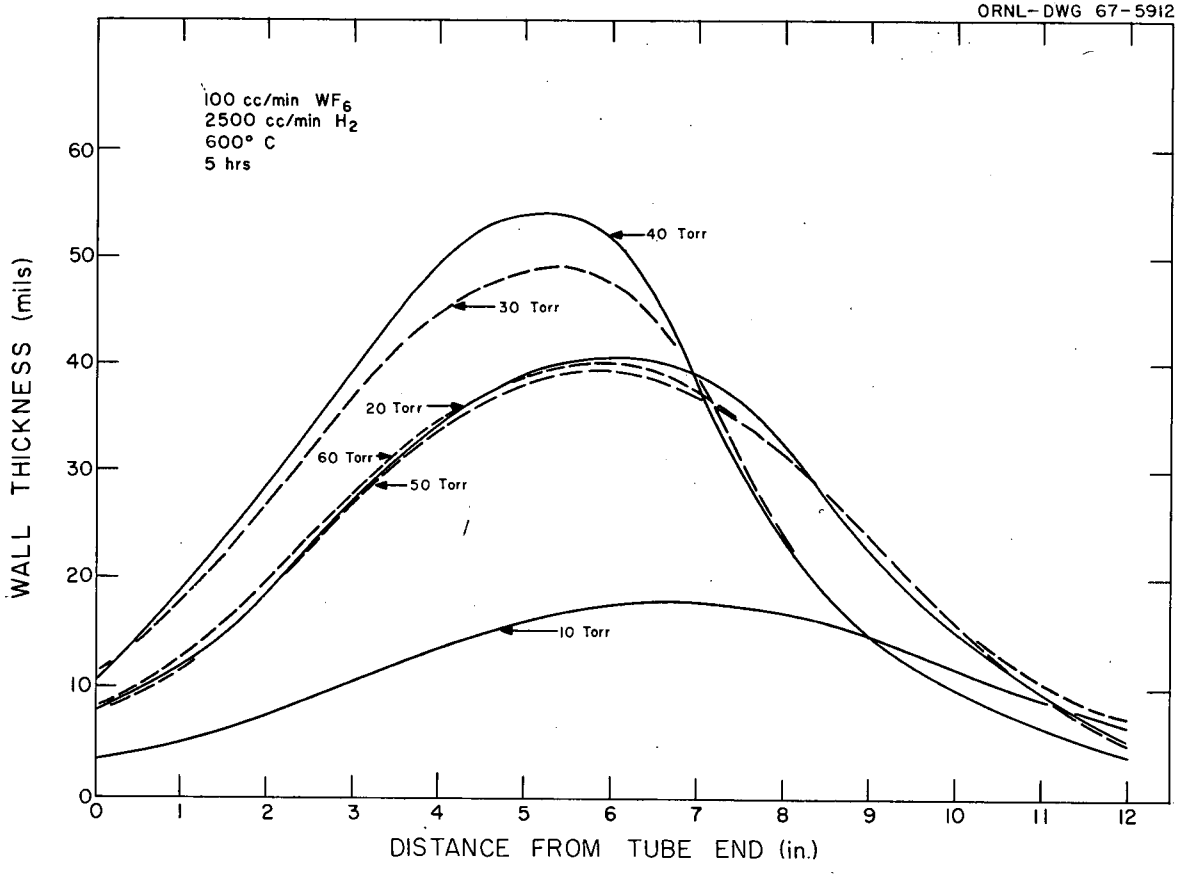

Fig. 3. Effect of Pressure on Tungsten Deposition.

tungsten, and a maximum was reached in the 40-torr run with a maximum thickness of 54 mils and an area of 0.343 in.^{2}. The 50- and 60-torr runs gave decreased amounts of deposit, approximately the amount deposited in the 20-torr run. Incipient nodule formation occurred in the 30- and 40-torr runs toward the exit end of the mandrel. This is shown in Fig. 4 for the 40-torr run. Figure 4(a) shows the velvety appearance of the "smooth" deposit, which has a very finely faceted surface. Figure 4(b) shows the surface of the same specimen at a point approximately 1.5 in. downstream from Fig. 4(a). Here, the surface is broken by a large number of cauliflower-like protuberances. We believe these to be the initial stages of nodule formation.

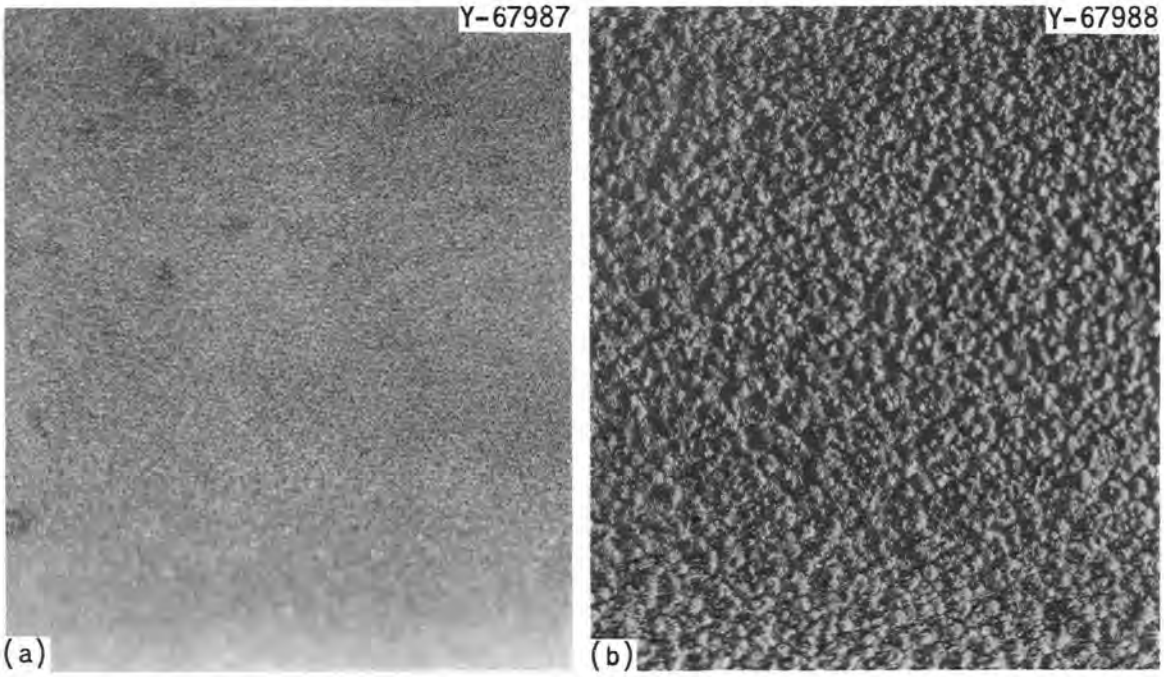

Fig. 4. Deposit Surfaces from Run 6 (100 cc/min WF_6, 2500 cc/min H_2, 40 torr). The poor focus at the top and bottom reflect the curvature of the surface. 9×. (a) Smooth area approximately 6 1/4 in. from inlet end of tube. (b) Nodular area approximately 7 3/4 in. from inlet end of tube.

Ratio Effects

Six runs were made at 100 cc/min WF_6, 20 torr, 600°C, and 5-hr duration. Figure 5 is a plot of deposit wall thickness versus position for several mole ratios. A H_2/WF_6 mole ratio of 10 resulted in little tungsten being deposited. A maximum thickness of approximately 16 mils was found with a longitudinal area of 0.132 in.^{2}. Mole ratios of 15 and 20 caused greater amounts of tungsten to be deposited. A maximum amount of deposit was obtained with a ratio of 25, which gave a maximum thickness of approximately 40 mils and an area of 0.298 in.^{2}. Further increases in the ratio caused the amount of tungsten deposited to decrease. Figure 6 is a plot of the integrated longitudinal area against mole ratio and illustrates

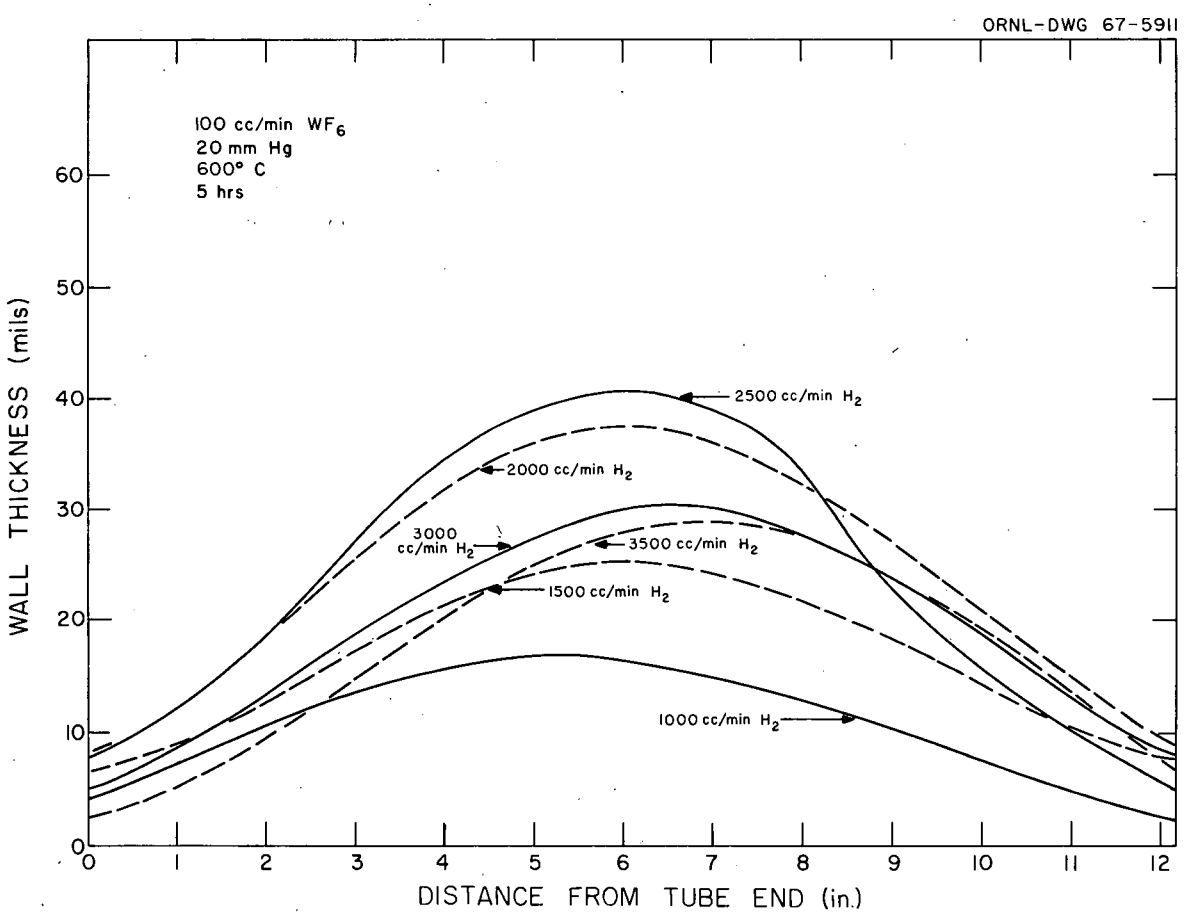

Fig. 5. Effect of Mole Ratio on Tungsten Deposition.

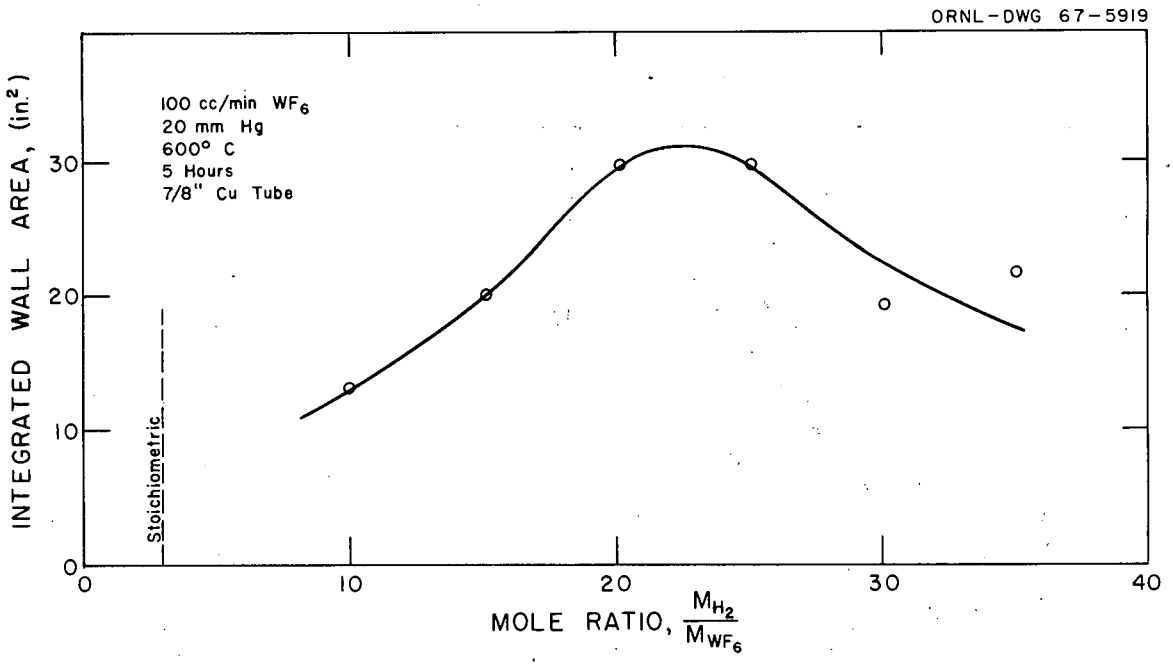

Fig. 6. Effect of Mole Ratio on the Amount of Tungsten Deposited.

the peaking and subsequent decrease of the amount deposited as the flow rate increased. Some values on the graph are averages of two runs. Similar results were obtained at other pressures.

Some method was needed for orderly plotting the data from the various runs to show the interactions of the deposition parameters. We were able to show this in Fig. 7, where the mass deposited is plotted against total flow rate; and in Fig. 8 where we plot the mass of tungsten deposited against a pressure-corrected total flow rate. The flow rate plotted in this manner is essentially, for a constant mandrel size, a measure of the gas velocity through the tube. As the system pressure is increased, the corresponding curves peak more sharply. This is in part caused by the manner in which the data are plotted (i.e., with a pressure term in the abscissa). Examination of Fig. 7, in which the mass of tungsten deposited is plotted as a function of total gas flow rate, shows that sharper peaks occur with increasing pressure. For clarity, no experimental points are shown. An increase in pressure for a given inlet flow rate increases the gas density and decreases the gas velocity.

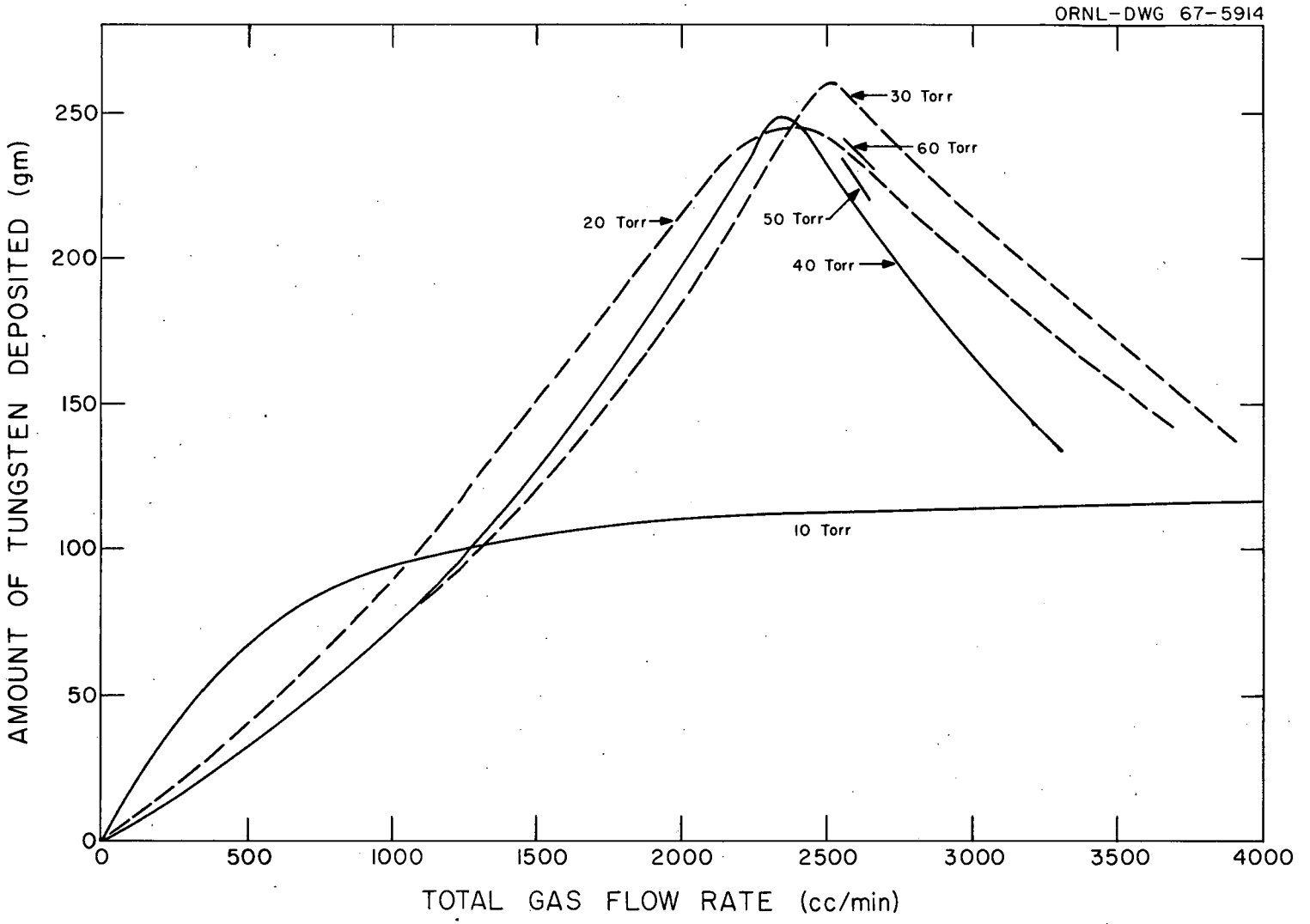

Fig. 7. Effect of Total Gas Flow Rate on the Mass of Tungsten Deposited.

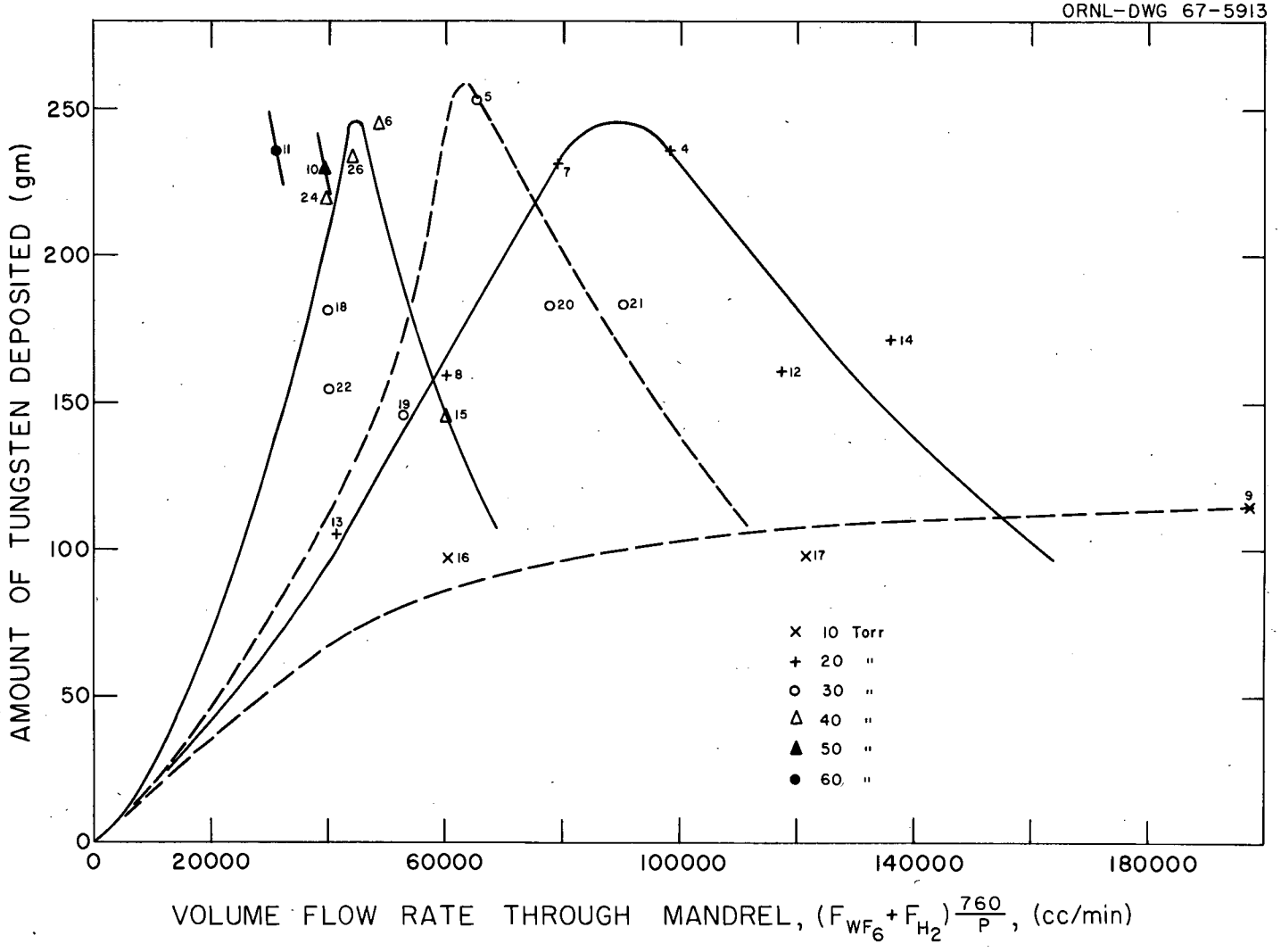

Fig. 8. Effect of Volume Flow Rate on the Mass of Tungsten Deposited. Numbers beside the points identify experiments in Tables 1 and 2.

Generally, there is an optimum recovery of tungsten associated with WF_6 flow rates below 100 cc/min and total flow rates around 2100 cc/min. Specifically, for total flow rates of 2100 cc/min, the recovery varies from approximately 26% for 300 cc/min WF_6 to approximately 46% for 200 cc/min WF_6, to approximately 90% for 100 cc/min WF_6, and to approximately 100% for all lower WF_6 flow rates.

Composition Effects on Nodule Formation

Examination of the face of a flat tungsten sheet, deposited inside a square-cross-sectioned mandrel, showed the transition from a relatively smooth surface to a nodular surface to be approximately parabolic with the parabola opening toward the inlet end of the mandrel, as shown in Fig. 9. Since the corners of a square-cross-sectioned mandrel create a drag on the gas stream and lower the gas velocity near them, the parabola is a velocity profile and the effects of temperature, composition, etc. are related to velocity.

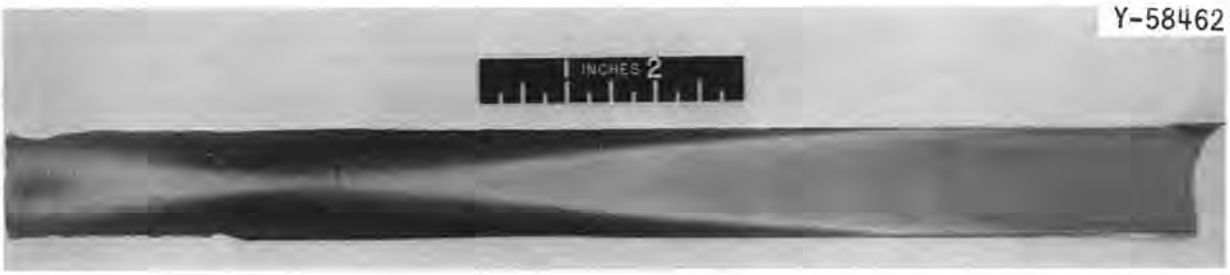

Fig. 9. Flat Tungsten Sheet Illustrating the "Parabolic" Transition Zone Between the Smooth and the Nodular Deposit. The gas flow was from right to left.

The basic premise of this discussion is that the formation of nodules is related to gas composition. This very general sentence takes into account such factors as diffusion rates of components, gas velocity through the tube, and reaction kinetics. All of these have a direct bearing on the gas composition <u>at the reaction surface</u> where the tungsten is being deposited. A basic assumption is now made that there is a specific gas composition, caused by WF_6 depletion, hydrogen fluoride blanketing, or

other factors, which could cause nodular growth to start on a particular set of lattice planes. The parabola could be, therefore, a line of constant gas composition at the reaction interface.

To show whether the texture of the deposit changed along the mandrel, a microfocus x-ray unit was used to obtain back-reflection Laue patterns of various portions of the deposited sheet.[6] The results did not indicate any change in growth plane in going from the smooth to the nodular formations. They did show that a very high preferred orientation was present in the deposit: ⟨100⟩ path normal to and parallel to the sheet and ⟨111⟩ direction normal to the pyramid facets.

Four x-ray patterns were taken of portions of the sheet. Two of these exposures were made on a pyramid-shaped growth inside the curve of the previously-mentioned parabola and the other two were made on a nodule downstream from the parabola. Figure 10 illustrates the positions of the exposures. Exposures 1 and 3 were made on the tops of the as-deposited

[6]J. C. Ogle, private communication to the author, June 3, 1965.

ORNL-DWG 67-5924

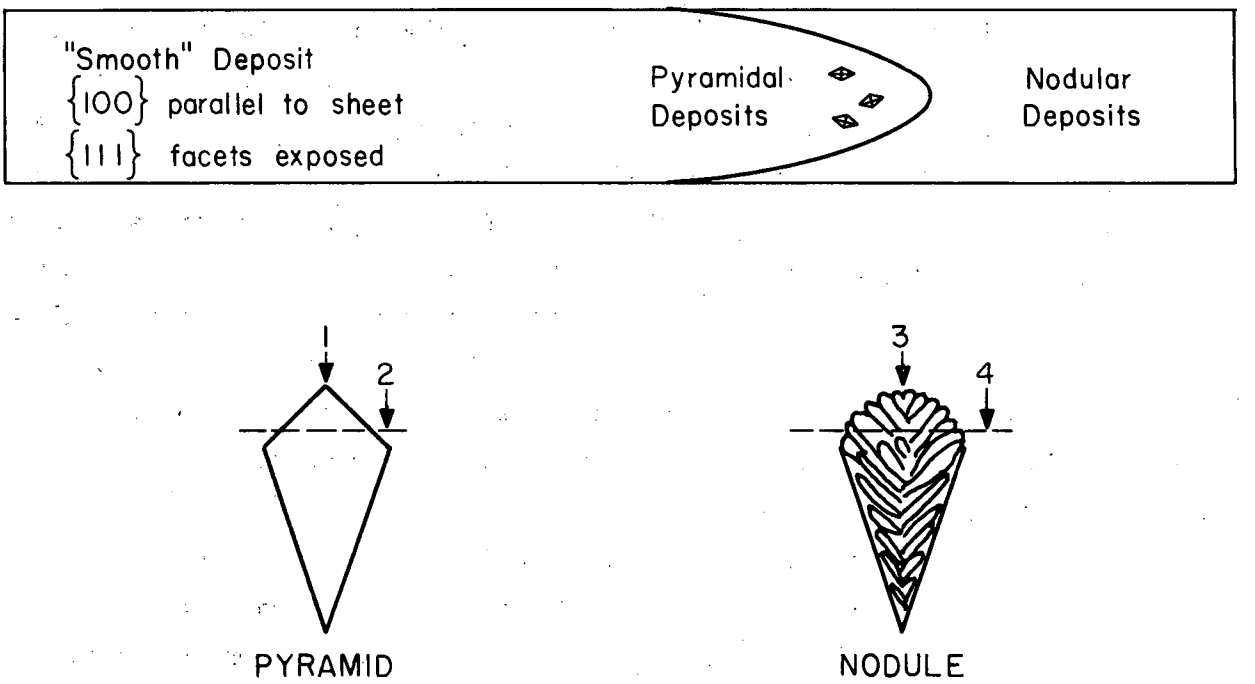

Fig. 10. Identification of Positions of Laue Back-Reflection Exposures.

pyramid and nodule, respectively. Exposures 2 and 4 were made on the same pyramid and nodule, respectively, after the tops had been polished and the remainder heavily etched. The Laue photographs are illustrated in Figs. 11 and 12. These photographs indicate that a very thin polycrystalline film is present on the surface of a single crystal in the case of the pyramid and on a coarser polycrystalline material in the case of the nodule.

Calculations show that a thickness of 7 μ of tungsten will reduce the intensity of a beam of x rays to 1% of its original value. Figure 11(a) shows both a randomly oriented fine-grained surface and from one to three grains below it. This surface layer cannot be much more than 7 μ thick, or else the single-crystal structure would be obscured. We hypothesize that this film was produced during the last few minutes of the deposition just after the WF_6 supply was turned off and the WF_6 concentration was decreasing. This hypothesis has far-reaching implications. Consider Fig. 13, which illustrates the following argument. The various regions found in the as-deposited sheet are shown together with a hypothetical steady-state WF_6 concentration variation along the sheet. We assume that there is a critical gas composition, indicated by the horizontal line on the graph, below which nodules can form. When the WF_6 supply value is closed at the end of a deposition run, the WF_6 composition does not immediately drop to zero. Instead, there is a rapid decrease in WF_6 concentration over a period of a minute or so before the residual WF_6 in the supply line is consumed. If the steady-state concentration gradient is as shown in the drawing, then lines A through E represent successive stages of WF_6 concentration after supply cutoff. Thus, the upstream portion of the deposit is exposed, at least momentarily, to the same gas concentrations that caused the downstream nucleation and growth of nodules. Such an exposure caused the formation of a thin coating of fine-grained material capable of producing the results seen in the Laue photographs.

To investigate the possibility that the thin film seen on the surface was a tungsten oxide, an x-ray diffractometer was used to obtain patterns of the surface of the sheet. Since only lines corresponding to pure tungsten were found, the diffraction rings seen in Figs. 11(a) and 12(a)

PHOTO 90015

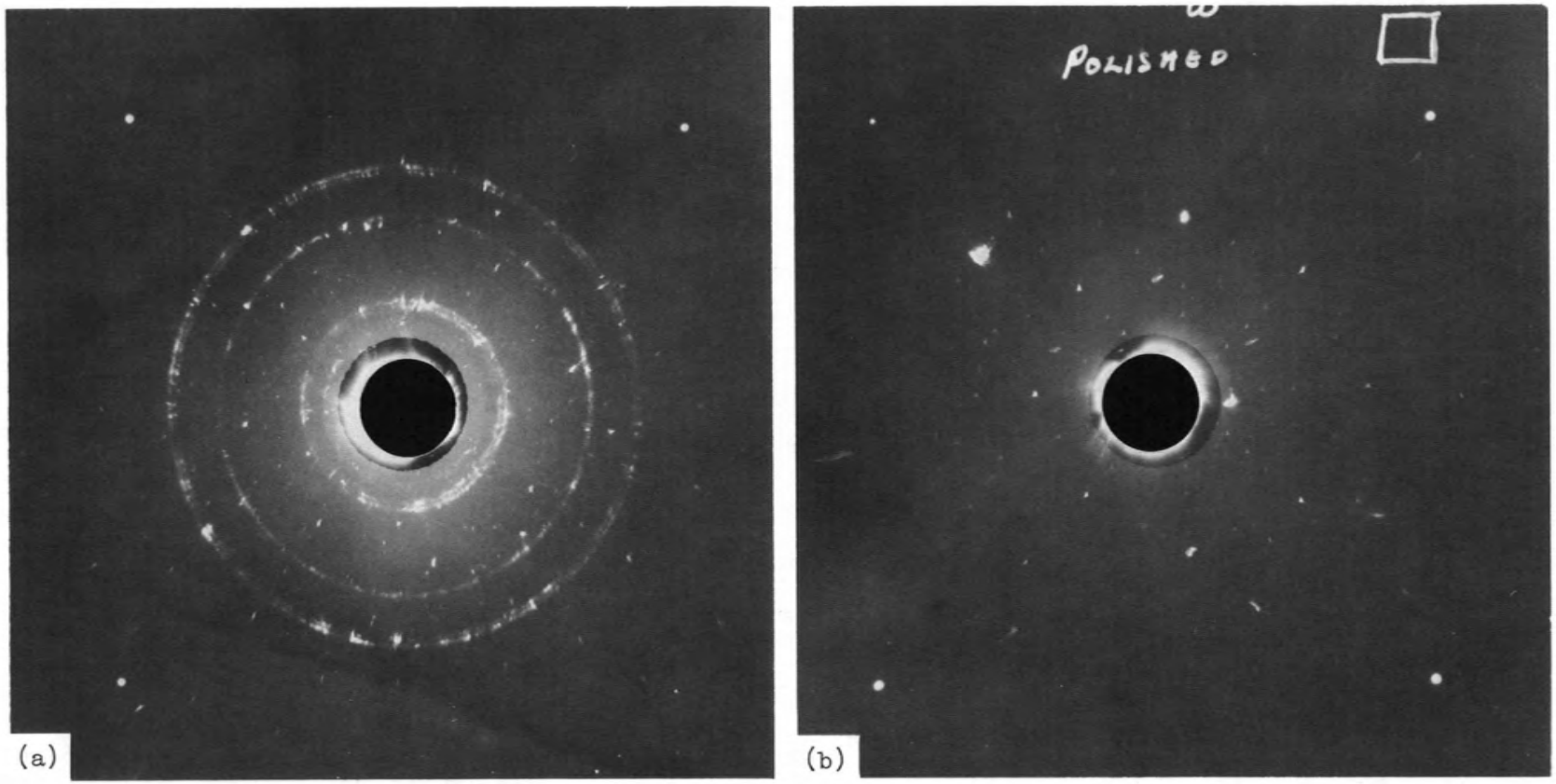

Fig. 11. Back-Reflection Laue Patterns of Pyramid from Region of Smooth Deposit. (a) Exposure 1, from tip, as deposited. (b) Exposure 2, as polished.

PHOTO 90016

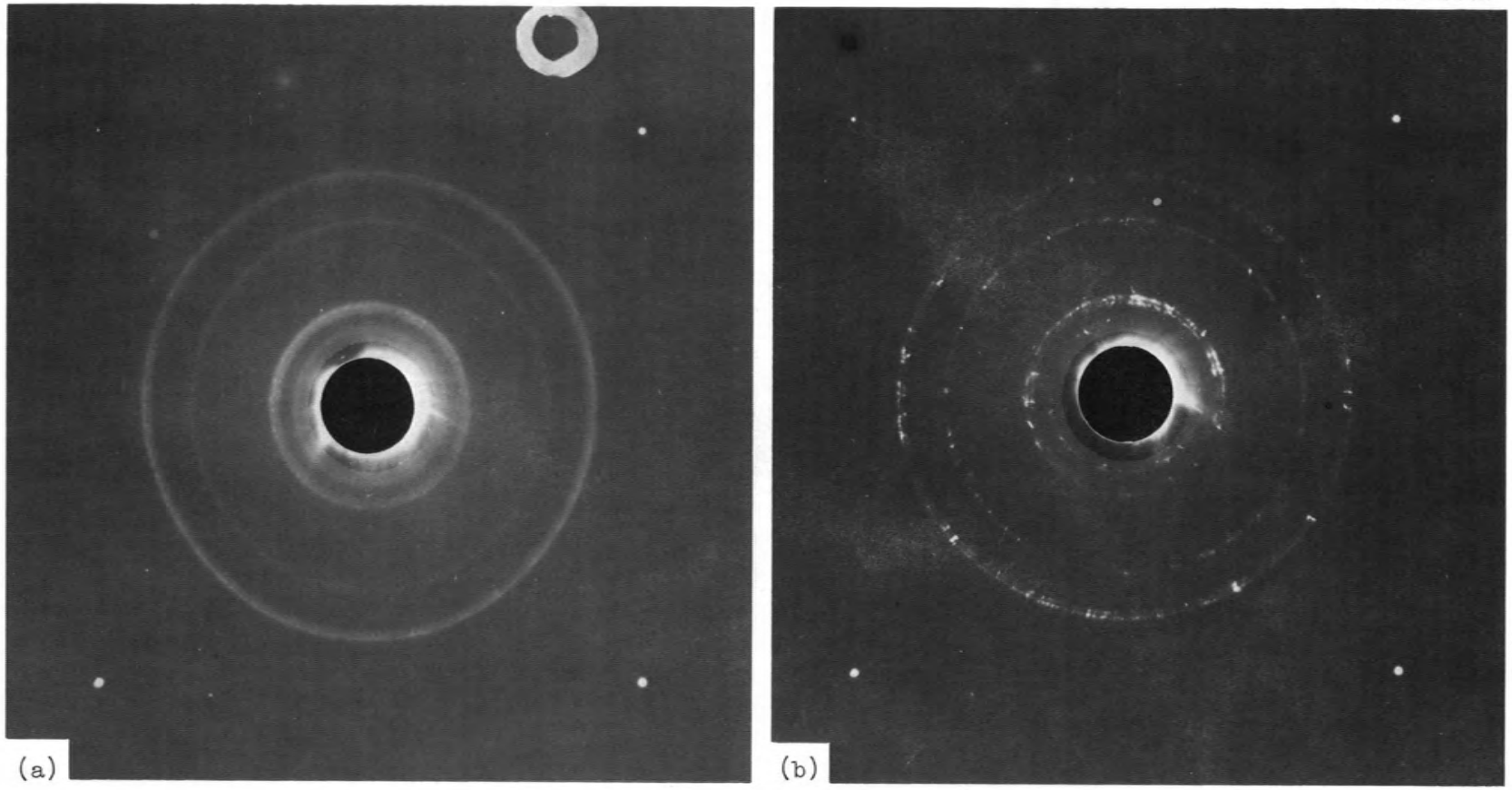

Fig. 12. Back-Reflection Laue Pattern of Nodule. (a) Exposure 3, from tip as deposited. (b) Exposure 4, as polished.

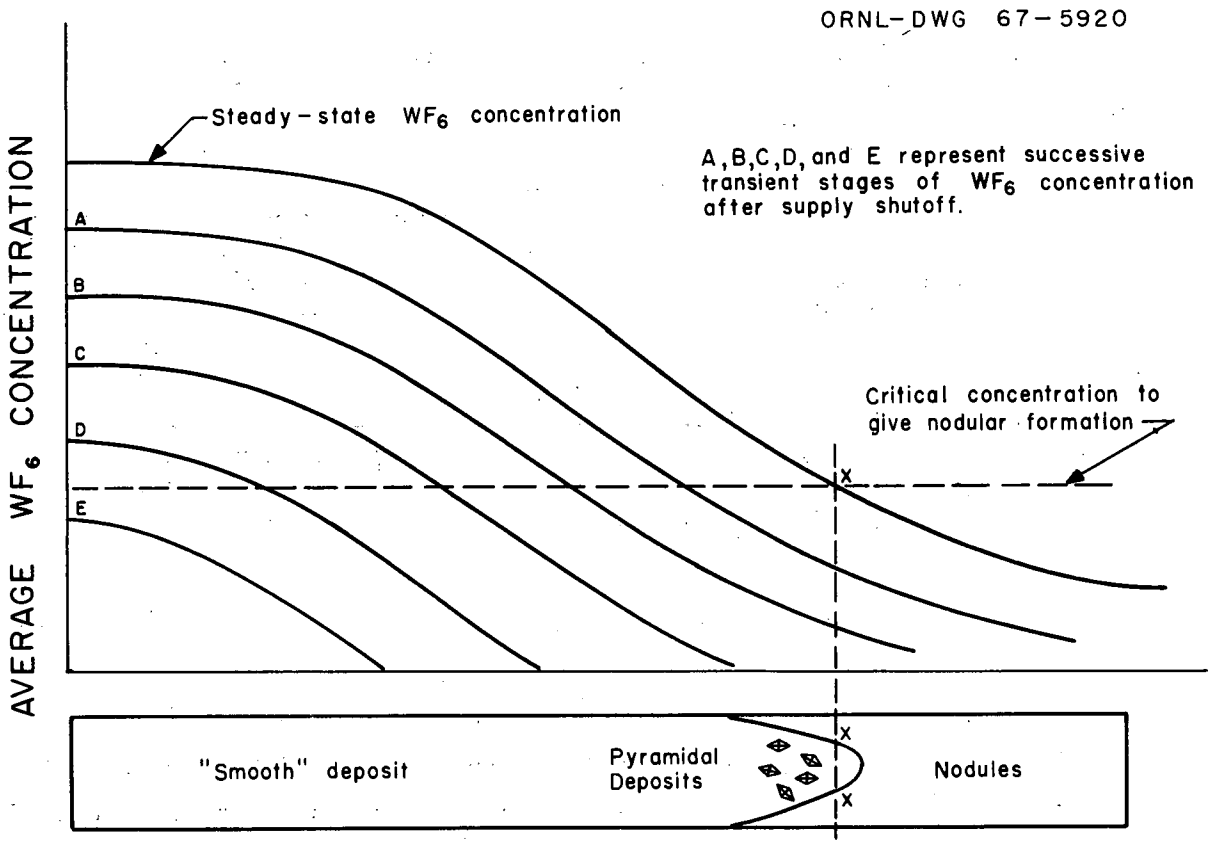

Fig. 13. Postulated WF_6 Concentration Curves as a Function of Position Along the Deposit.

were from tungsten and not from an oxide. The diffractometer confirmed the preferred orientation of the deposit to be predominantly (100) parallel to the surface. A semiquantitative analysis of the diffractometer traces, using the peak heights as an indication of preferred orientation, yielded the information shown in Table 3.

These results clearly show that the smooth surface of the sheet has a highly developed texture with the (100) plane parallel to the surface of the sheet. The nodular portion of the surface has a much less well developed orientation of the (100) plane, with the peak height of the (100) plane only approximately four times its height for the random material. A second diffractometer run showed the [100] direction to be concentrated largely within an angle of ±5° from the normal of the sheet. This was verified by finding a high concentration of [110] directions near an angle 45° from the normal to the sheet.

Table 3. Results of the X-Ray Diffractometer Traces on the Surface of the As-Deposited Tungsten Sheet

(hkl)	Relative Intensity		
	Random Material[a]	"Smooth Surface" (inside the parabola)	"Nodular Surface" (outside the parabola)
(110)	100	100	100
(200)	15	80,000	60

[a]X-Ray Powder Data File Sets 1–5 (Revised), Am. Soc. Testing Mater. Spec. Publ. 48-J (1960), J. V. Smith et. al., eds., American Society for Testing Materials, Philadelphia.

Figure 14 shows the faceted appearance of the surface of the "smooth" material in a high-magnification electron micrograph.

In addition to the surface layers of nodules and pyramids in the deposit, two other layers were present in the sheet. One layer next to the mandrel consisted of a fine-grained deposit less than 5 mils thick. It could have been formed at a higher temperature than the rest of the deposit, since it was in close contact with the hot copper mandrel. Such proximity could have caused a very rapid nucleation from the gas phase and hence the fine-grained appearance. The fine grain size could also be the result of an epitaxial relationship with the mandrel.

Another layer formed directly on the previous layer. This consisted of a columnar layer approximately 20 mils thick. We postulate that the critical gas composition for producing nodules or pyramids is very temperature dependent. As the deposit increased in thickness, the longer path for heat transfer combined with the cooling effects of the gas stream caused the temperature at the deposition surface to decrease. At a certain thickness, determined by deposit thickness and gas concentration, the nodular or pyramidal growths began.

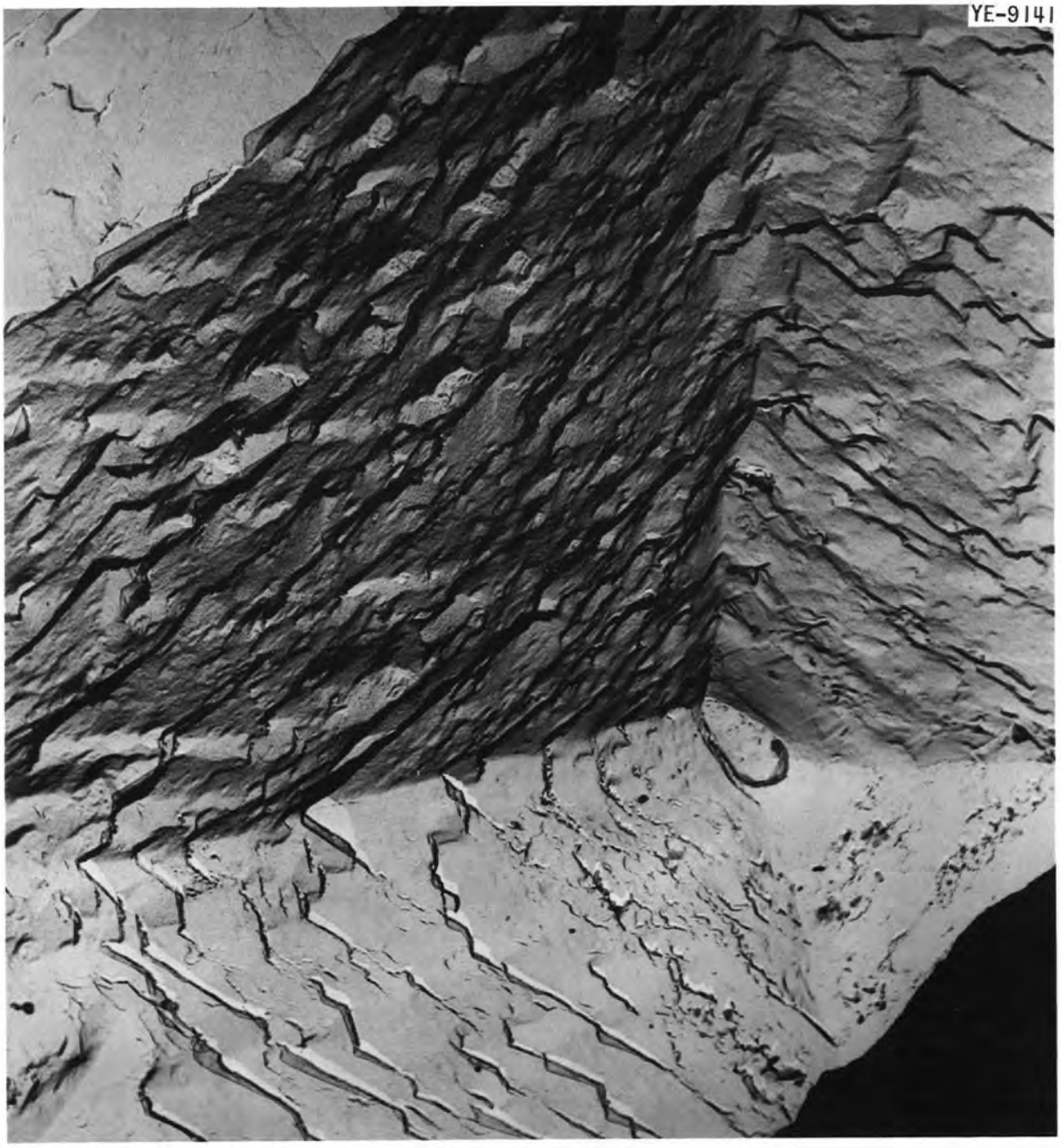

Fig. 14. Typical Facet on the "Smooth" Surface of the Deposit. Note the pyramidal shape.

The possibility of nucleation in the gas phase being the cause of nodule formation has been discussed by both Campbell[7] and Fleming.[8] It is hard to rationalize gas-phase nuclei as being able to produce such a sharply delineated line as the parabola exhibits, whereas a reaction that occurred either on or at the gas-metal interface could produce such a structure. Impurities in the system might also cause the formation of nodules. Again, however, it is hard to conceive of a leak, either real or virtual, as being the cause of the demarcation line. The line is too sharp and too reproducible.

EXTRAPOLATION AND THEORY

The experimental results reported herein are by no means the whole story of tungsten deposition. They are experimentally accurate in what they cover but are somewhat lacking in scope and range of deposition variables. We do not discuss here well-supported findings but analyze some possibilities for relating observed deposition experience to theory to stimulate more definitive experimental work on tungsten deposition. Additional experimental results, not reported in previous sections of the report will be brought into elucidate some of the hypotheses.

As a basis for discussion, Fig. 15 is a hypothetical extension of Fig. 8. The pressure curves approximate the experimental curves, and the assumption is made that the temperature, time, mandrel size, and WF_6 flow rate are held constant throughout all runs. We reaffirm that the values plotted on the abscissa are equivalent to gas velocity through the mandrel.

The line dividing the region of nodule formation from that of no nodule formation is based on four empirical observations and some deductions arrived at from a study of individual deposition curves. In the deposit near the exit ends of the mandrel, runs 5, 6, 11, and 26 showed structural

---

[7]W. B. Campbell, Feasibility of Forming Refractory Fibers by a Continuous Process, 3rd Quart. Progr. Rept. Aug. 25 to Nov. 25, 1963, AMRA-CR-63-03/3.

[8]J. D. Fleming, Consultant from Georgia Institute of Technology, Letter to R. L. Heestand, Aug. 15, 1964.

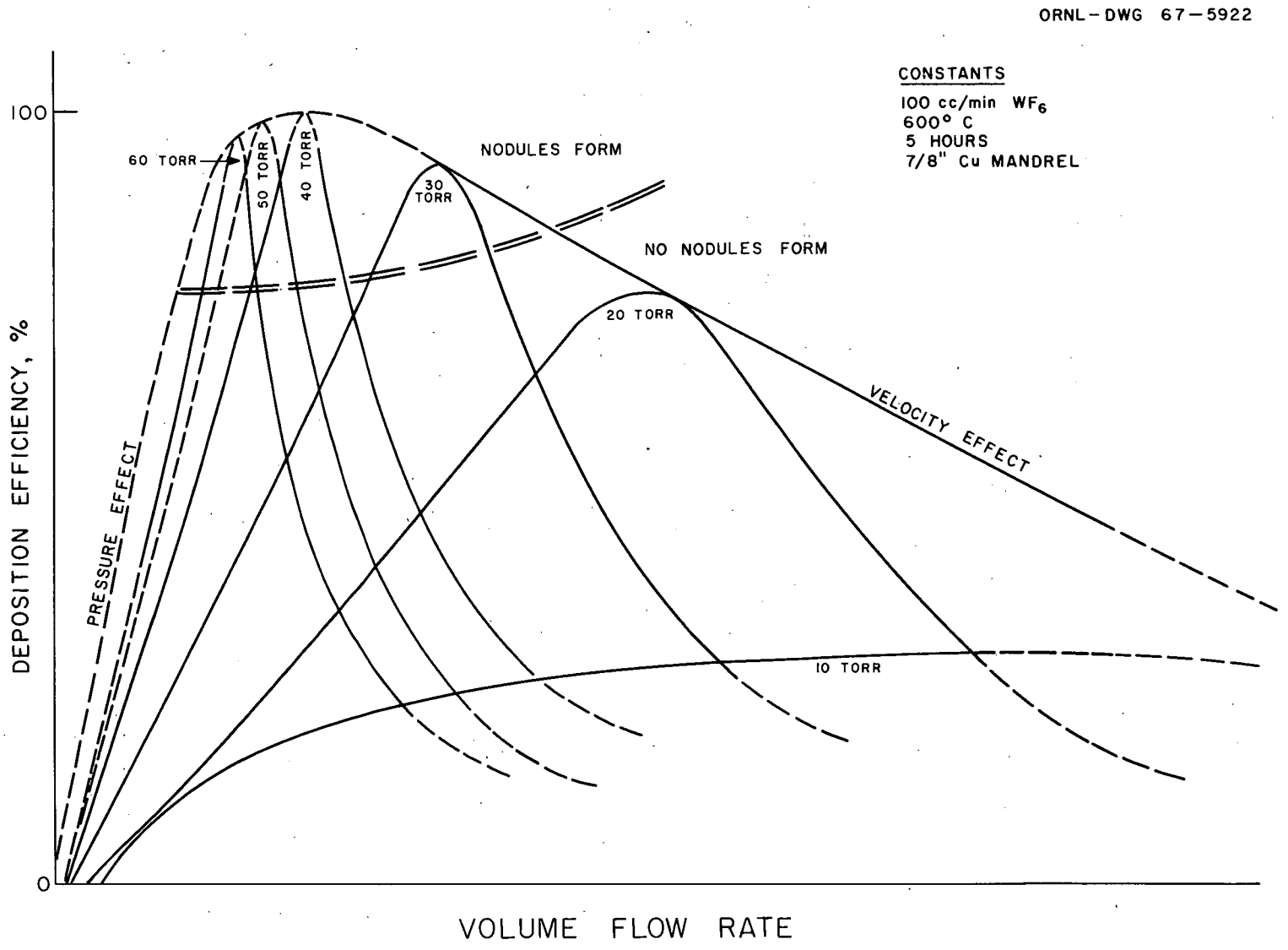

Fig. 15. Hypothetical Extension of Fig. 8.

changes that can be interpreted as incipient nodule formation. Figure 4 illustrates the basis of this interpretation. These runs formed the heaviest deposits found in any of the 100-cc/min runs. Plots of amount deposited against distance from tube end show a high peak before the mid-point of the mandrel and then a rapid decrease in deposit thickness in the second half of the tube. This decrease corresponded to the area in which the incipient nodulation was observed. We postulate that the susceptibility to nodulation is dependent upon the gas composition in the region where WF_6 has been depleted by a rapid reaction rate.

Pressure and Envelope Curves

Many hypotheses can be derived concerning the shapes and sizes of the pressure and envelope curves associated with the deposition process. A study of Fig. 15 shows that an envelope curve can be drawn through the peaks of the deposition curves. We postulate that the high-pressure region (the positive slope portion) of the curve is related thermodynamically to the effect of pressure on a system that reacts with a net increase in the number of moles of gas. We also feel that the negative slope portion of the envelope is related to the mechanical transport of gas through the tube at too high a velocity for complete reaction to occur. The lower the pressure, the higher is the gas velocity through the tube and, correspondingly, the less time there is for the reaction to take place. For constant WF_6 flow rate, time, temperature, and mandrel size with a range of pressures, the envelope represents the maximum amount of tungsten that can be deposited. The "velocity-effect" slope is believed to be sensitive to mandrel diameter. A large mandrel diameter would decrease the velocity of the gas and allow time for the reaction to approach equilibrium. This would result in a nearly horizontal slope of the envelope to the right of the peak. Conversely, a small tube diameter would force the gas to a high velocity and the efficiency would be greatly affected. The resulting envelope curve would show a rapid decrease in the amount of tungsten deposited.

The "pressure effect" or positive-slope portion of the envelope should go through the origin at infinite pressure. The individual pressure curves should cut the abscissa as shown in Fig. 16. At zero hydrogen flow there would be no deposit of metal. There would, however, still be 100-cc/min WF_6 flowing. This metered flow rate, when multiplied by 760/P, gives the point where the pressure curve cuts the abscissa.

It is interesting to speculate on the effects of changing the WF_6 flow rate on the envelope around the pressure curves. A few runs were made at WF_6 flow rates of 80, 100, 200, and 300 std cc/min. The system pressure was 20 torr; the hydrogen flow rate was adjusted to compensate for the

ORNL-DWG 67-5921

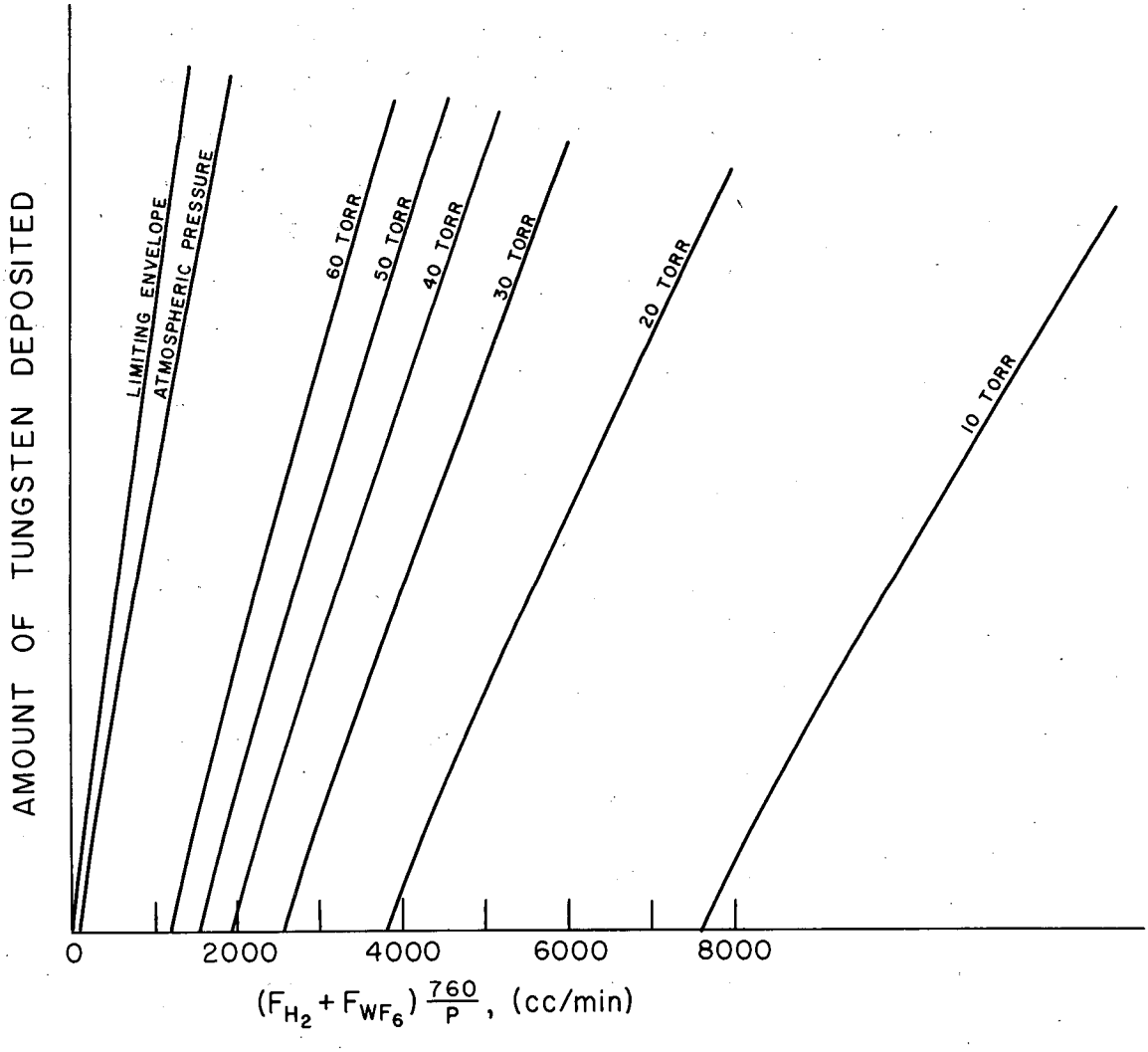

Fig. 16. Effect of Volume Flow Rate on Tungsten Deposition.

additional WF_6 to give a constant value on the abscissa, and the mandrel size was held constant. One run was also made with a WF_6 flow rate of 40 std cc/min in which the hydrogen was not adjusted to give the same abscissa value as the other runs. The results of these runs are shown as points in Fig. 17. The amount of tungsten deposited increased from the 40 std cc/min to the 100 std cc/min flow rate and then decreased as the higher flow rates were used. The curves in Fig. 17 are an attempt to rationalize this behavior. It should be emphasized that these are constant-pressure curves and not envelope curves. Logic tells us that, up to a point, the amount of tungsten deposited should increase with increasing WF_6 flow rate. Then, if the WF_6 and hydrogen flow rates are held at a constant sum, the amount of deposit should decrease due to the lack of sufficient hydrogen to consume the excess of WF_6. We believe that the curves shown here represent the effects that would be obtained by varying the H_2/WF_6 ratio for each of the WF_6 flow rates at constant pressure and mandrel size. The diverging positive-slope portions of the lines are an effect of Le Chatelier's principle. The larger the H_2/WF_6 ratio, the greater is the abundance of hydrogen present and, therefore, the greater is the driving force for completion of the reaction. At a H_2/WF_6 ratio of

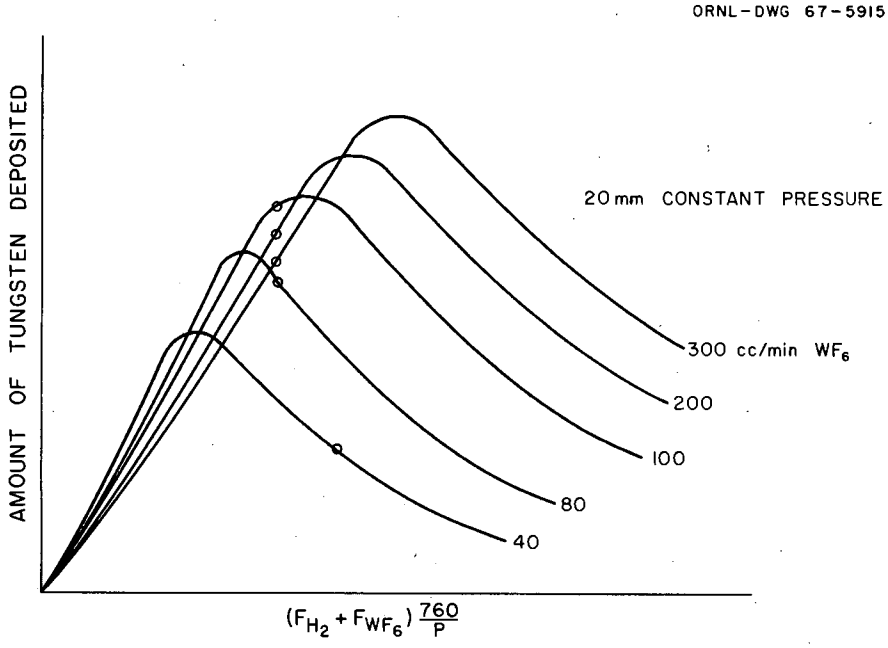

Fig. 17. Deposition Curves Reflecting Differences in WF_6 Flow Rate.

zero, the curves cut the abscissa at points proportional to the flow rate of WF_6. There should be an optimum ratio, dependent upon WF_6 flow rate and mandrel geometry, that would give maximum efficiency.

Having postulated the shape of the pressure curves corresponding to various flow rates of WF_6, let us now consider what the envelopes could look like in relation to the pressure curves. Consider the peaks of the pressure curves that pass through the four points in Fig. 17. These peaks lie on separate envelopes, for which we should be able to estimate the positions. Figure 18 shows our working hypothesis, which is analyzed below.

Within certain limits, an increase in the amount of WF_6 introduced into the system will generally result in an increase in the amount of tungsten deposited. For this to be true, however, the flow rate of hydrogen must be optimized. The upper limit of this increase is probably

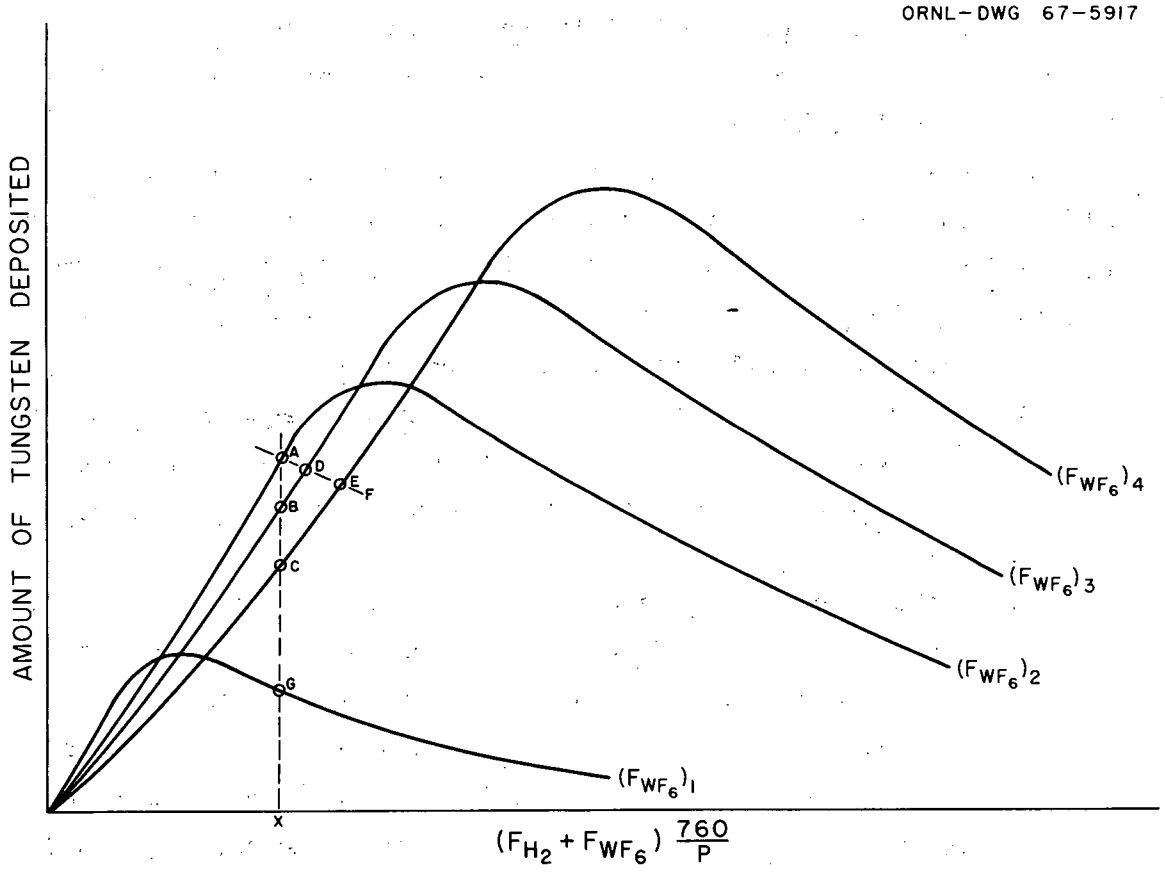

Fig. 18. Schematic Deposition Envelopes.

fixed by system geometry. Consider a point near the peak of a constant pressure curve. If the WF_6 flow rate were increased by a small amount and the hydrogen flow rate decreased by a like amount, the amount deposited should increase, and the resultant point should lie above the previous point on a vertical line on the plot. The pressure curve through this new point is one of a series bounded by a new envelope, characteristic of the higher WF_6 flow rate. We have seen from the results and conjecture given in Fig. 17 that the pressure curve peaks for various flow rates of WF_6 do not fall in a vertical line above each other but, instead, are displaced to the right with increasing flow rates. By definition, the envelope of each curve will be tangent to that curve at a point near the peak. As a first assumption, we postulate equal slopes for the geometry-dependent, or negative-slope, portions of the envelopes. We know that the envelope curves pass through the origin. What remains is to guess at the positive-slope or thermodynamically dependent portions of the envelope curves.

Again, Le Chatelier's principle can be used to qualitatively place the curves in their proper order. All references are to the letters and lines shown in Fig. 18.

Assume a vertical line, AX, characteristic of constant $(F_{WF_6} + F_{H_2})$ and P. Assume point A to represent almost complete reaction of the available WF_6 by the high excess of hydrogen. If $(F_{WF_6})_2 < (F_{WF_6})_3 < (F_{WF_6})_4$, then $(H_2/WF_6)_2 > (H_2/WF_6)_3 > (H_2/WF_6)_4$. Under the conditions of constant total flow rate the H_2/WF_6 ratio would decrease to zero (point X), if the WF_6 flow rate were to continue to increase until it equaled the total flow rate. The amount of tungsten deposited under that condition would, obviously, be zero. Points B and C represent, therefore, conditions of progressive hydrogen starvation.

If, on the other hand, the WF_6 flow rate were allowed to decrease toward zero and the hydrogen flow rate allowed to increase to equal the total flow rate, then eventually the amount of deposit would again decrease to zero. A condition intermediate to these can be represented by an envelope in which the peak is to the left of the vertical line AX and below point A. The amount of tungsten deposited would be shown by point G.

At low flow rates (to avoid having to include geometry effects), let $(H_2/WF_6)_2 = (H_2/WF_6)_3 = (H_2/WF_6)_4$ and P = constant. Let $(F_{WF_6})_2 < (F_{WF_6})_3 < (F_{WF_6})_4$. These conditions correspond to a nonvertical line AF extending to the right through point A. Each point other than point A has a nearer optimum hydrogen content than its analogous point in the previous example (i.e., D is better than B, and E is better than C).

Since there is a pressure variable in the abscissa, we should be able to bring points D and E back to the vertical line through A by increasing the system pressure. Thermodynamically, the equilibrium in the reaction $WF_6 + H_2 \rightarrow W + 6HF$ should be forced to the left. This would further justify the position of B and C under A.

We believe Fig. 18 to be a good qualitative representation of the positions and shapes of the envelopes corresponding to various flow rates of WF_6. Two other configurations of envelopes, shown in Figs. 19 and 20, can be considered. Figure 19, which shows the envelopes branching from a common curve, is not applicable since it cannot follow the thermodynamic argument given above. Figure 20, which shows the envelopes not crossing, is also incapable of a thermodynamic explanation of the positive-slope portion of the curves. At low WF_6 flow rates and constant pressure, the higher hydrogen flow rate should give lower efficiency. Or, in other words,

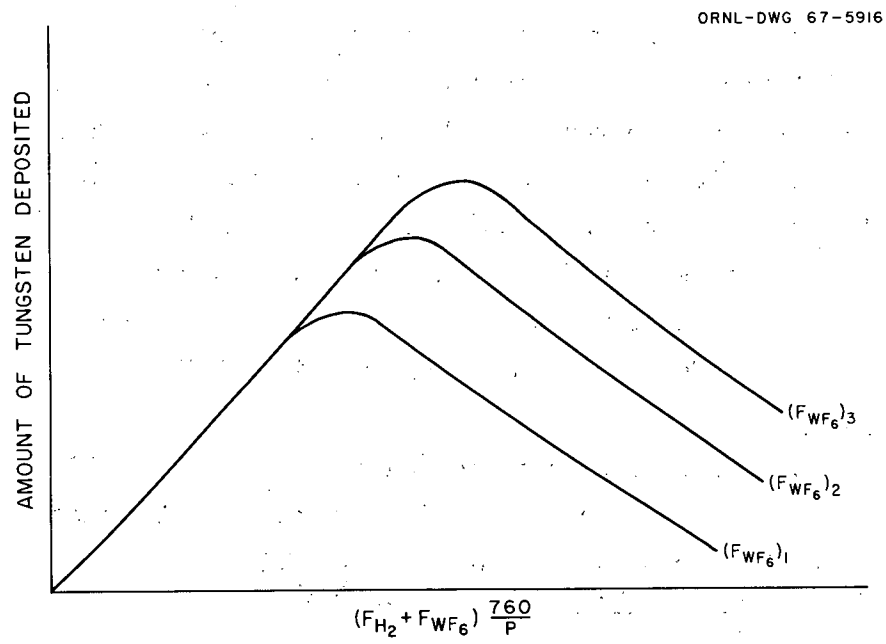

Fig. 19. Postulated Envelopes Branching from a Common Curve.

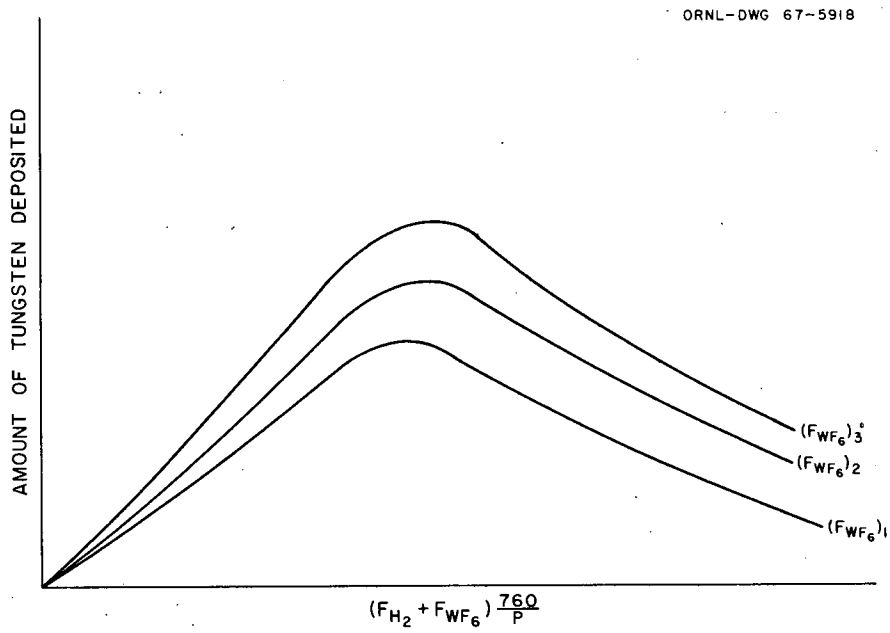

Fig. 20. Postulated Envelopes Not Crossing.

if the sum of the flow rates is a constant, an increasing H_2/WF_6 ratio should give points on a vertical line below the point corresponding to the lowest H_2/WF_6 ratio.

Effects of Type of Gas Flow Pattern

An interesting theory has been related by Robinson,[9] who has studied work done by others[10,11] on the flow patterns of heavy gases. One has always assumed that the gases in the deposition system follow a laminar flow pattern. This is not necessarily so. Barber[10] reported that the heavy WF_6 gas may flow turbulently at Reynolds numbers as low as 15, and he calculated that this is well within the flow ranges used in this study. Hydrogen and hydrogen fluoride, on the other hand, behave like normal gases and require Reynolds numbers approaching 2000 before exhibiting

---

[9] W. C. Robinson, private communication, March 3, 1965.

[10] E. J. Barber, private communication to W. C. Robinson.

[11] A. L. Myerson and J. H. Eicher, "The Viscosity of Gaseous Uranium Hexafluoride," J. Am. Chem. Soc. 74, 2758–2761 (1952).

turbulent flow. Robinson contends that the entrance conditions of the gas, where WF_6 is present in large concentrations, may cause a region of turbulent flow and that downstream, where the WF_6 has been depleted, the gas stream requires a much higher Reynolds number for turbulent flow. This Reynolds number is not available and the flow is laminar. Once laminar flow is established, the hydrogen fluoride evolved by the reaction may be forced to stay close to the deposition surface, since gross mixing or convection currents are no longer in the gas stream. Thus the surface would see a hydrogen fluoride blanket, which would require that the remaining WF_6 and hydrogen diffuse to the surface. The sudden secession of turbulent flow would greatly magnify the gradual composition change that has been taking place down the tube and could in turn produce a sharp transition between the smooth and nodular deposits.

The above theory in no way disagrees with the concept of the parabola being analogous to a velocity profile. Knowing that the Reynolds number is directly related to velocity, if we assume that the smooth deposit is obtained under turbulent conditions, then the higher the velocity, the farther down the tube the smooth region should extend. Figure 21 shows a qualitative representation of the changes in composition and Reynolds number down the length of the tube. The above arguments have assumed a constant temperature down the length of the mandrel. Actually, there is a gradual temperature increase down the length of the tube from the inlet to the outlet. However, the effect of this gradient on the Reynolds number should be negligible, since the viscosity and hence the Reynolds number are fairly independent of temperature for changes of less than 50°C. Temperature changes could affect such phenomena as diffusion rate, surface energy, and gas volume.

To illustrate the foregoing hypotheses, consider the effects of efficiency on the tendency for nodule formation. We have shown experimentally that high efficiencies increase the tendency for the formation of nodules. This can be explained as the result of two reinforcing effects. There is a great depletion of the WF_6 and concomitant enhancement of the hydrogen fluoride content of the gas stream. There may also be a change from turbulent to laminar flow due to an increase in the Reynolds number required for turbulent flow. The combined effect is that the downstream

ORNL-DWG 67-5923

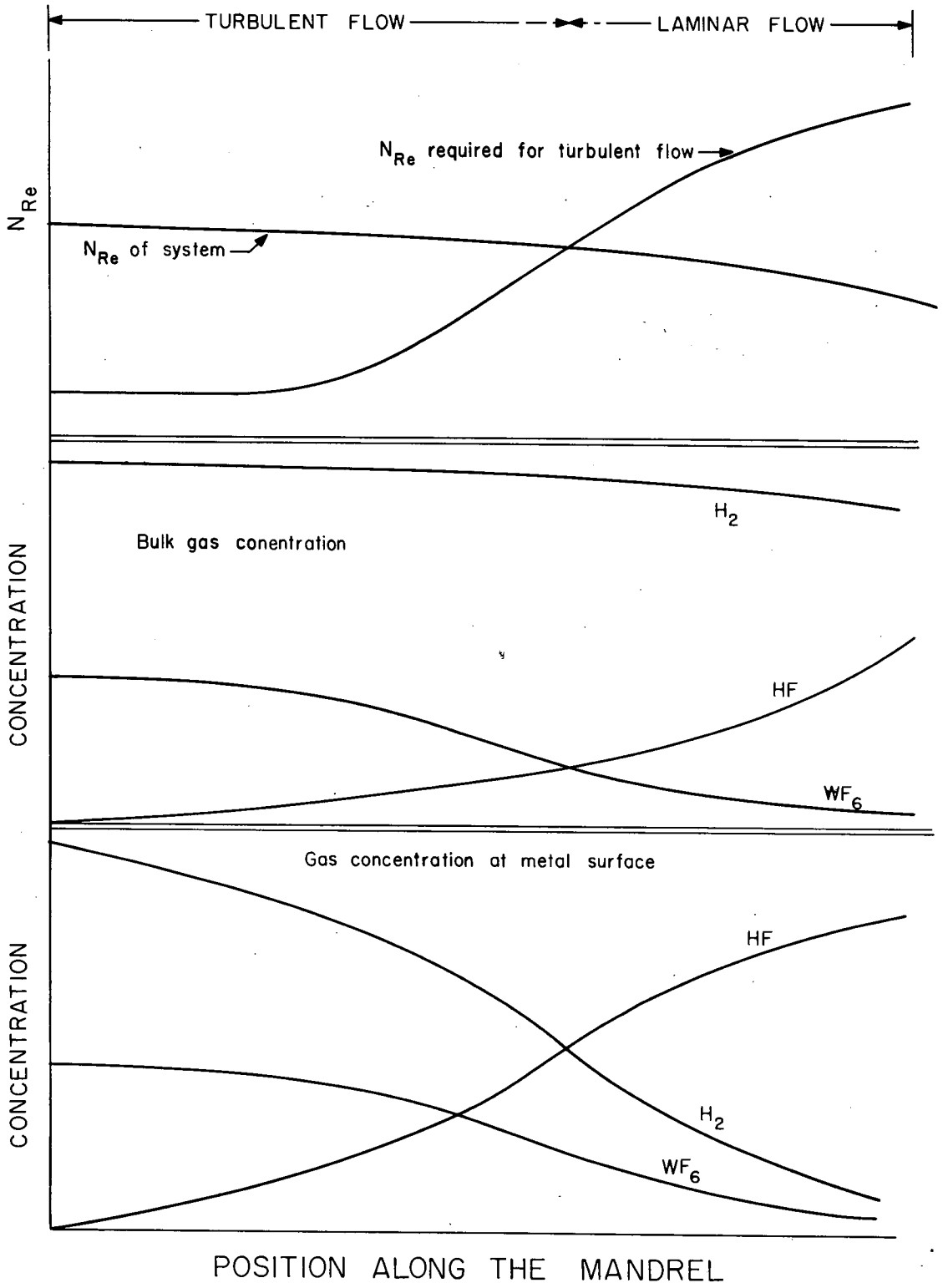

Fig. 21. Qualitative Representation of Composition Changes and Reynolds Number Along the Tube.

deposition surface sees very little WF_6, and nodulation takes place. Consider now a less efficient run. Assuming the same inlet conditions as before, the WF_6 will be less depleted with length and the remaining WF_6 may keep the critical Reynolds number low and the flow turbulent. Thus, the downstream surface sees a greater concentration of WF_6 and nodulation is not obtained.

CONCLUSIONS

The process of tungsten deposition was amenable to a systematic study of deposition parameters. Careful attention to the control of the parameters gave both reproducible and predictable deposition behavior.

The amount of tungsten deposited was a function of a number of variables, the most important of which are pressure, WF_6 flow rate, total flow rate, and mandrel shape and size. Temperature is an important variable, but it was held nominally constant during this study.

Incipient nodule formation was seen in high-efficiency runs. This indicated that WF_6 depletion and hydrogen fluoride enrichment at the surface, due to a number of causes, were largely responsible for the change in deposit morphology.

The rather limited exploration of deposition parameters in this study enabled us to postulate qualitative relationships among the parameters. These relationships included the effects of flow rate on the amounts of tungsten capable of being deposited at a given pressure and total flow rate, the effects of higher pressure than those used in the study, and the effect of mandrel geometry on the amount of tungsten deposited. The most important benefit derived from such qualitative results is the ability to predict in what direction an effect will shift due to a change in a parameter. For this reason, this work can be used as a guideline for more detailed quantitative work to follow.

Generally, for a given mandrel size and system pressure, there was an optimum WF_6 flow rate and H_2/WF_6 ratio for which the efficiency or amount of tungsten deposited was a maximum. Changes in mandrel size or system pressure should require a change in gas flow rates and ratio to again achieve maximum deposits.

ACKNOWLEDGMENTS

We are grateful to W. C. Robinson, J. D. Fleming, J. V. Cathcart, and J. I. Federer for many helpful discussions on the art of pyrolytic tungsten deposition. Special thanks are extended to Robinson and Federer for their criticisms and suggestions concerning this report. We wish to thank E. R. Turnbill for construction and maintenance of the experimental apparatus and for making many of the deposition runs discussed in this report. Many thanks are extended to J. C. Ogle of the Structure of Metals Group of the Metals and Ceramics Division for his work and discussions on the orientation of the deposited tungsten. The ability of his equipment to produce an extremely well collimated x-ray beam was a great help in producing his valuable radiographs.

Acknowledgment is due the staff of the Metals and Ceramics Division Reports Office and Glenn C. Nelson for their help in producing this report.

INTERNAL DISTRIBUTION

1–3. Central Research Library
4–5. ORNL – Y-12 Technical Library
Document Reference Section
6–15. Laboratory Records Department
16. Laboratory Records, ORNL R.C.
17. ORNL Patent Office
18. G. M. Adamson, Jr.
19. G. E. Boyd
20. F. L. Culler
21. J. E. Cunningham
22. C. W. Dean
23. J. H. DeVan
24. R. G. Donnelly
25. J. I. Federer
26. J. H Frye, Jr.
27. J. L. Gregg
28. W. O. Harms
29–31. M. R. Hill
32–36. D. O. Hobson
37. T. S. Lundy
38. H. G. MacPherson
39. W. R. Martin
40. R. E. McDonald
41. D. L. McElroy
42. C. J. McHargue
43. P. Patriarca
44. G. A. Reimann
45. P. L. Rittenhouse
46. W. C. Robinson
47. A. C. Schaffhauser
48. S. H. Smiley (K-25)
49. R. L. Stephenson
50. D. A. Sundburg

EXTERNAL DISTRIBUTION

51. J. H. Burson, Georgia Institute of Technology
52. D. F. Cope, RDT, SSR, AEC, Oak Ridge National Laboratory
53. J. D. Fleming, Georgia Institute of Technology
54. C. W. Gorton, Georgia Institute of Technology
55. R. L. Heestand, Battelle Memorial Institute, Columbus, Ohio
56. W. R. Holman, Lawrence Radiation Laboratory
57. W. J. Larkin, AEC, Oak Ridge Operations
58. C. F. Leitten, Jr., Linde Division, Union Carbide Corp.
59. F. H. Patterson, Battelle Memorial Institute, Columbus, Ohio
60. L. W. Roberts, Lawrence Radiation Laboratory
61. J. M. Simmons, AEC, Washington
62. J. E. Spruiell, University of Tennessee
63. E. E. Stansbury, University of Tennessee
64. M. J. Whitman, AEC, Washington
65. Laboratory and University Division, AEC, Oak Ridge Operations
66–80. Division of Technical Information Extension